AFRL-AFOSR-VA-TR-2019-0319

Estimation of Shape and Relative Motion for Partially Resolved Objects

Jason Gross
West Virginia University Research Corporation

06/03/2019
Final Report

Air Force Research Laboratory
AF Office Of Scientific Research (AFOSR)/ RTB1
Arlington, Virginia 22203
Air Force Materiel Command

REPORT DOCUMENTATION PAGE	*Form Approved* *OMB No. 0704-0188*

1. REPORT DATE *(DD-MM-YYYY)*: 28-05-2019

2. REPORT TYPE: Final Report

3. DATES COVERED *(From - To)*: Apr 2015 - Apr 2019

4. TITLE AND SUBTITLE

(YIP) Estimation of Shape and Relative Motion for Partially Resolved Objects in Optically Acquired Imagery

5a. CONTRACT NUMBER

5b. GRANT NUMBER

FA9550-15-1-0215

5c. PROGRAM ELEMENT NUMBER

6. AUTHOR(S)

Gross, Jason (acting PI)
Christian, John A. (original PI and final report author)
Postdocs: Jagat, Ashish
Graduate students: Rhodes, Andrew P.; Ertl, Christopher A.; Puritz, Jacob

5d. PROJECT NUMBER

5e. TASK NUMBER

5f. WORK UNIT NUMBER

7. PERFORMING ORGANIZATION NAME(S) AND ADDRESS(ES)

West Virginia University Research Corporation, 886 Chestnut Ridge, Morgantown, WV 26505
Rensselaer Polytechnic Institute, 110 8th Street, Troy, NY 12180

8. PERFORMING ORGANIZATION REPORT NUMBER

9. SPONSORING/MONITORING AGENCY NAME(S) AND ADDRESS(ES)

Air Force Office of Scientific Research
875 NORTH RANDOLPH STREET, RM 3112
ARLINGTON VA 22203-1954

10. SPONSOR/MONITOR'S ACRONYM(S)

11. SPONSOR/MONITOR'S REPORT NUMBER(S)

12. DISTRIBUTION/AVAILABILITY STATEMENT

Approved for public release; distribution unlimited

13. SUPPLEMENTARY NOTES

Dr. Christian was proposing PI. After moving to RPI in 2017, Dr. Gross became acting PI at WVU. Bulk of remaining technical work was subcontracted to Dr. Christian at RPI for completion

14. ABSTRACT

This work aimed to advance 2D image and 3D mesh processing techniques for partially resolved space objects. Over the course of this project, we made advancements in the following areas: construction of a 3D scale space and finding salient features (keypoints) in this scale space, graph-based methods for matching keypoints of a newly observed object with a catalog of known objects, 3D shape modeling from sequences of silhouette images, recognition of a partially resolved object in a 2D image with a convolutional neural network, analytic corrections for bearing bias of partially resolved objects.

15. SUBJECT TERMS

Navigation, Space imaging, Scale space

16. SECURITY CLASSIFICATION OF: a. REPORT	b. ABSTRACT	c. THIS PAGE	17. LIMITATION OF ABSTRACT	18. NUMBER OF PAGES	19a. NAME OF RESPONSIBLE PERSON
U	U	U	SAR	10	John Christian

19b. TELEPHONE NUMBER *(Include area code)*: 518-276-8024

Standard Form 298 (Rev. 8/98)
Prescribed by ANSI Std. Z39.18

INSTRUCTIONS FOR COMPLETING SF 298

1. REPORT DATE. Full publication date, including day, month, if available. Must cite at least the year and be Year 2000 compliant, e.g. 30-06-1998; xx-06-1998; xx-xx-1998.

2. REPORT TYPE. State the type of report, such as final, technical, interim, memorandum, master's thesis, progress, quarterly, research, special, group study, etc.

3. DATE COVERED. Indicate the time during which the work was performed and the report was written, e.g., Jun 1997 - Jun 1998; 1-10 Jun 1996; May - Nov 1998; Nov 1998.

4. TITLE. Enter title and subtitle with volume number and part number, if applicable. On classified documents, enter the title classification in parentheses.

5a. CONTRACT NUMBER. Enter all contract numbers as they appear in the report, e.g. F33315-86-C-5169.

5b. GRANT NUMBER. Enter all grant numbers as they appear in the report. e.g. AFOSR-82-1234.

5c. PROGRAM ELEMENT NUMBER. Enter all program element numbers as they appear in the report, e.g. 61101A.

5e. TASK NUMBER. Enter all task numbers as they appear in the report, e.g. 05; RF0330201; T4112.

5f. WORK UNIT NUMBER. Enter all work unit numbers as they appear in the report, e.g. 001; AFAPL30480105.

6. AUTHOR(S). Enter name(s) of person(s) responsible for writing the report, performing the research, or credited with the content of the report. The form of entry is the last name, first name, middle initial, and additional qualifiers separated by commas, e.g. Smith, Richard, J, Jr.

7. PERFORMING ORGANIZATION NAME(S) AND ADDRESS(ES). Self-explanatory.

8. PERFORMING ORGANIZATION REPORT NUMBER. Enter all unique alphanumeric report numbers assigned by the performing organization, e.g. BRL-1234; AFWL-TR-85-4017-Vol-21-PT-2.

9. SPONSORING/MONITORING AGENCY NAME(S) AND ADDRESS(ES). Enter the name and address of the organization(s) financially responsible for and monitoring the work.

10. SPONSOR/MONITOR'S ACRONYM(S). Enter, if available, e.g. BRL, ARDEC, NADC.

11. SPONSOR/MONITOR'S REPORT NUMBER(S). Enter report number as assigned by the sponsoring/ monitoring agency, if available, e.g. BRL-TR-829; -215.

12. DISTRIBUTION/AVAILABILITY STATEMENT. Use agency-mandated availability statements to indicate the public availability or distribution limitations of the report. If additional limitations/ restrictions or special markings are indicated, follow agency authorization procedures, e.g. RD/FRD, PROPIN, ITAR, etc. Include copyright information.

13. SUPPLEMENTARY NOTES. Enter information not included elsewhere such as: prepared in cooperation with; translation of; report supersedes; old edition number, etc.

14. ABSTRACT. A brief (approximately 200 words) factual summary of the most significant information.

15. SUBJECT TERMS. Key words or phrases identifying major concepts in the report.

16. SECURITY CLASSIFICATION. Enter security classification in accordance with security classification regulations, e.g. U, C, S, etc. If this form contains classified information, stamp classification level on the top and bottom of this page.

17. LIMITATION OF ABSTRACT. This block must be completed to assign a distribution limitation to the abstract. Enter UU (Unclassified Unlimited) or SAR (Same as Report). An entry in this block is necessary if the abstract is to be limited.

Final Report

Estimation of Shape and Relative Motion for Partially Resolved Objects in Optically Acquired Imagery

Award No: FA9550-15-1-0215

Air Force Office of Scientific Research (AFOSR)
Young Investigator Program (YIP)

28 May 2019

Dr. Jason Gross (acting PI)
West Virginia University
1306 Evansdale Drive
Morgantown, WV 26506
Email: Jason.Gross@mail.wvu.edu

Final report prepared by:
Dr. John A. Christian (original PI)
Rensselaer Polytechnic Institute
110 8th Street
Troy, NY 12180
Email: chrisj9@rpi.edu

1 Introduction

Basic research in the science of image processing and estimation theory is necessary to lay the theoretical foundations for future U.S. Department of Defense capabilities that rely on information extracted from imagery. One such capability of particular interest is the ability to robustly detect, characterize, and track resident space objects (RSOs). Systems must be capable of achieving these objectives using passive sensors (e.g., cameras) at a variety of ranges, lighting conditions, viewing geometries, and other operational constraints. To this end, a great deal of research has been performed on extracting information from unresolved observations of RSOs using information such as light curve data and advanced modeling/estimation techniques. Likewise, a host of algorithms (ranging from feature extraction to optical flow) are available for inferring information from images containing a fully resolved RSO. What is missing, however, is a thorough understanding of how the maximum amount of information may be extracted from images of partially resolved RSOs. As objects that are far away become closer, they will typically begin as an unresolved object, then transition to a partially resolved object, and eventually become a fully resolved object. Such an evolution of images is common during on-orbit proximity operations or rendezvous. An example of this type of transition is shown graphically in Fig. 1. Obtaining the maximum amount of information as quickly as possible allows for better decision-making earlier in an encounter.

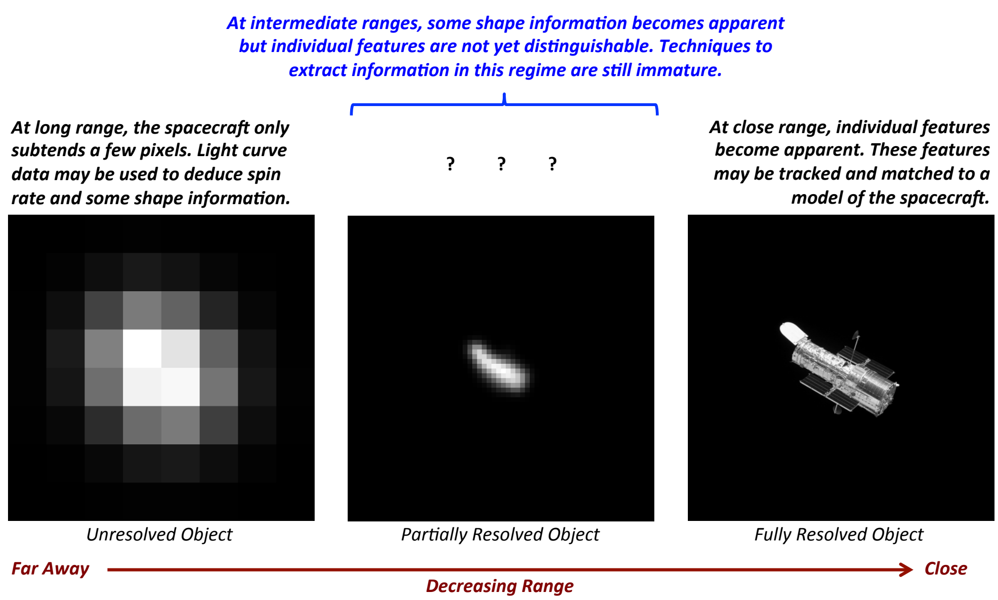

Figure 1: Objects move from unresolved (left image), to partially resolved (middle image), to fully resolved (right image) during a typical on-orbit rendezvous.

Over the course of this Young Investigator Program (YIP) award, we have made progress in a number of critical areas related to the understanding and use of partially resolved imagery. The key results generated by our research team lie in three areas:

1. Partially resolved object shape modeling and description
2. Partially resolved object recognition
3. Relative navigation (RelNav) with partially resolved objects

The sections that follow summarize our key results in each of these three areas.

2 Summary of Results in Partially Resolved Object Shape Modeling and Description

2.1 3D Scale-Space and Keypoint Detection

2.1.1 3D Scale-Space

Of all the various topics we investigated as part of this YIP award, the analysis and description of an object's 3D shape from a scale-space perspective consumed (by far) the most time and effort. This effort is motivated by the simple fact that the progression of an object from unresolved to partially resolved to fully resolved during an on-orbit rendezvous mirrors closely the construction of a classic image scale space. The difficulty, of course, is that the observed object's appearance changes during the rendezvous (due to attitude changes, lighting changes, etc.). This ultimately led us to the idea of building a scale space directly on a 3D model instead of the projection of that 3D model onto a particular image.

Scale-space construction methods on 3D surfaces may be separated into two categories: (1) the diffusion of vertex locations and (2) the diffusion of a signal along the surface. The first type is analogous to the diffusion of not only the pixel intensities, but also the pixel locations of a 2D image. This may lead to mesh shrinkage and non-physical deformations. Instead, diffusion of a signal along the surface is analogous to holding the pixel locations constant, and diffusing the signal. We, therefore, focused primarily on methods where the vertex locations are held constant.

Scale-space is governed by the diffusion equation and implemented with discrete approximations [1, 2]. The in-surface isotropic diffusion equation

$$\frac{\partial u}{\partial t} = \alpha \nabla^2_{\mathcal{S}} u \tag{1}$$

constructs a scale-space on 3D surfaces, where u is a function defined on the surface, t is the diffusion time (related to the scale-parameter), α is the constant of diffusion, and $\nabla^2_{\mathcal{S}}$ is the continuous Laplace-Beltrami operator (LBO) which is a generalization of the Laplace operator to surfaces. The characteristic solution (i.e., the impulse response) to Eq. 1 is sometimes referred to as the heat kernel [3], which is the well-known Gaussian used for 1D signal analysis [1, 4] and 2D image scale-space [5, 6]. For surfaces embedded in $\mathbb{R}^3$, the solution to the diffusion equation is less straightforward.

Discretization in space of Eq. 1 requires a discrete approximation to the LBO, the most common of which are the umbrella [7], cotangent [8, 9], mesh [10]. Diversity in LBO construction occurs because no discrete LBO can satisfy all natural properties of the continuous Laplacian [11, 12]. We built pipelines for constructing a 3D scale space with each of these LBOs.

In addition to studying various discrete LBOs for solving Eq. 1 on explicit surfaces, we also spent considerable effort investigating diffusion on implicit surfaces. Specifically, we considered implicitly representing the surface as level sets [13], signed distance fields (SDF) [14], or closest point representations (CPR) [15]. These methods are agnostic to inhomogeneous mesh representations because they embed the explicit surface on a grid in a one-dimensional higher space on which the classic Cartesian definitions of gradient and divergence with well-studied numeric techniques apply. Most of our effort in this area focused on CPR, since this approach can handle open or closed, non-orientable, and higher dimensional surfaces. We implemented the implicit closest point method (ICPM) from [16] to construct a scale-space on surfaces. After a detailed study, we ultimately found implicit methods to require too much memory and computational expense for reasonable deployment in spaceflight applications. Hence, most of the remaining discussions focus exclusively on solutions with explicit surfaces.

2.1.2 3D Keypoint Detection

Once a 3D scale-space has been built, we must search this scale-space for stable and salient keypoints. These keypoints exist at all scales from fine (corresponding to fully resolved) to coarse (corresponding to partially resolved). Clearly, we have most interest in the coarse keypoints here — although the fine keypoints are just as useful if this concept is extrapolated to fully resolved imagery.

Amongst the group of classic keypoint detectors, finding extrema in the scale-normalized Laplace of Gaussian (LoG), $t\nabla^2$G, generally provides the most stable keypoints [17]. The LoG is computationally expensive, but may be closely approximated with the Difference of Gaussians (DoG). Begin with the discretization of Eq. 1 in time with a Gaussian as

$$\frac{\mathrm{G}_{n+1} - \mathrm{G}_n}{t_{n+1} - t_n} \approx \alpha \nabla^2_{\mathcal{S}} \mathrm{G} \tag{2}$$

Assuming we step through the scale space according to $t_{n+1} = k^2 t_n$, for the scale-normalized LoG leads to

$$\mathrm{DoG} = \mathrm{G}_{n+1} - \mathrm{G}_n \approx (t_{n+1} - t_n)\, \alpha \nabla^2_{\mathcal{S}} \mathrm{G} = (k^2 - 1)\alpha t_n \nabla^2_{\mathcal{S}} \mathrm{G}$$

where $(k^2 - 1)\alpha$ is a constant over all scales, thus not affecting extrema detection. With a scale-space signal, the DoG is calculated as

$$\mathrm{D}(\mathbf{u}) = \mathbf{u}_{n+1} - \mathbf{u}_n \tag{3}$$

where D is short for the DoG and also utilized by SIFT [6], MeshDoG [18], GSS [19], and others.

Vertices whose DoG value achieves an extrema relative to their neighbors in the current level, and the levels immediately below and above, are selected as keypoints. The keypoints' scales are automatically selected from the level of the scale-space stack at which the extrema exists.

Example keypoints generated by the different LBOs are shown in Fig. 2. Keypoints are shown as red spheres, with the sphere diameter representing the scale. We generally find that the mesh LBOs exhibit better repeatability than the umbrella or cotangent LBOs. This can be seen in Fig. 3, where the primary metric of concern is *relative repeatability*.

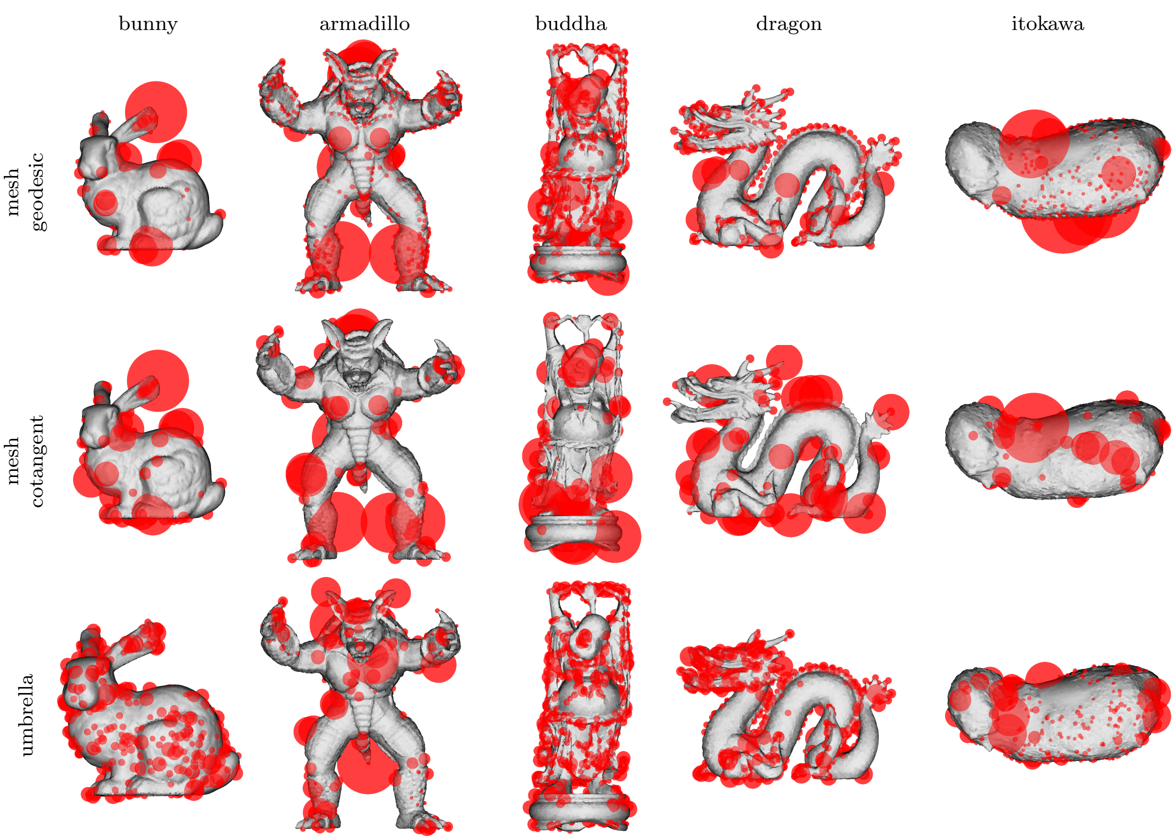

(a) $m_{\mathbf{v}} = 34834$, $m_f = 69451$, $\bar{e} = 1.00$

(b) $m_{\mathbf{v}} = 50002$, $m_f = 100000$, $\bar{e} = 1.92$

(c) $m_{\mathbf{v}} = 24939$, $m_f = 49886$, $\bar{e} = 5.21$

(d) $m_{\mathbf{v}} = 24956$, $m_f = 49899$, $\bar{e} = 4.49$

(e) $m_{\mathbf{v}} = 39998$, $m_f = 79992$, $\bar{e} = 1.3993$

Figure 2: Visualization of keypoints (denoted by red spheres) on five different reference models using different methods of diffusion. Models (a)-(d) are from the Stanford 3D Scanning Repository, `http://graphics.stanford.edu/data/3Dscanrep/`. Model (e) is from [20].

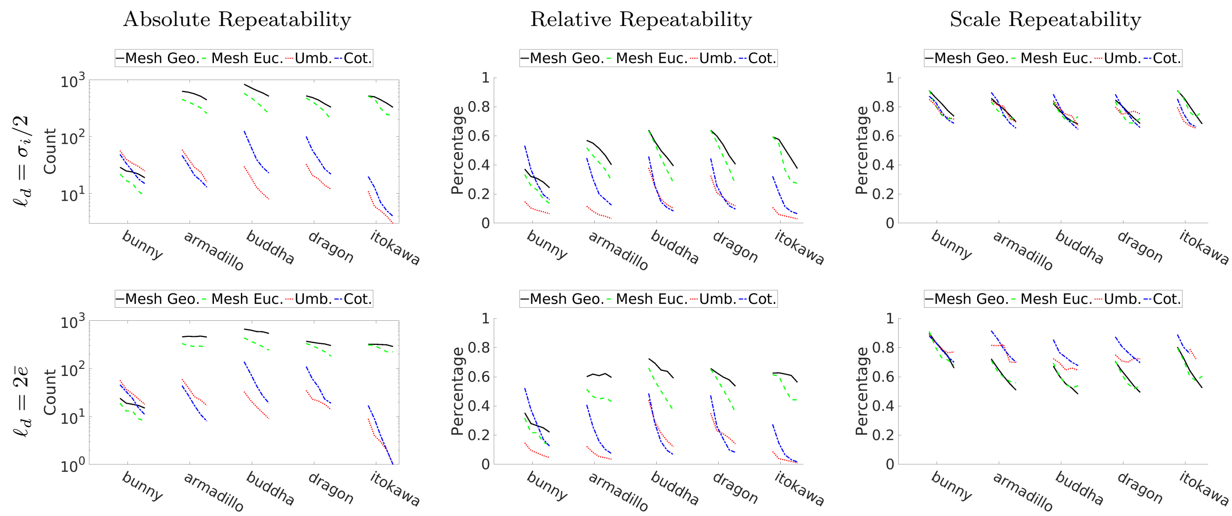

Figure 3: Keypoint repeatability results when adding Gaussian noise to the vertex locations and recomputing the mean curvature signal. Plots show median repeatability values from Monte Carlo simulation at five different levels of vertex noise (increasing noise left to right). Results are presented for two different methods fo selecting the distance threshold ℓ_d used to determine keypoint repeatability.

2.2 Shape from Silhouette (SfS)

In situations where the relative attitude is known, it is possible to build a 3D model using an observed object's silhouette in an ensemble of images collected from varying vantage points. This procedure is often called shape from silhouette (SfS). We implemented a straightforward sphere carving technique that performs well so long as the object's size is single-valued along each radial direction (injective to the sphere). Example results given synthetic images of a satellite are shown in Fig. 4.

During the course of this project, we also explored the use of exact polyhedral visual hulls (EPVH) [21]. We had some limited success with this approach, but substantially more effort is required to fully develop this pipeline. In early 2019, we also briefly explored silhouette-based shape representation in curvature scale space [22], and hope to continue this line of investigation in future work.

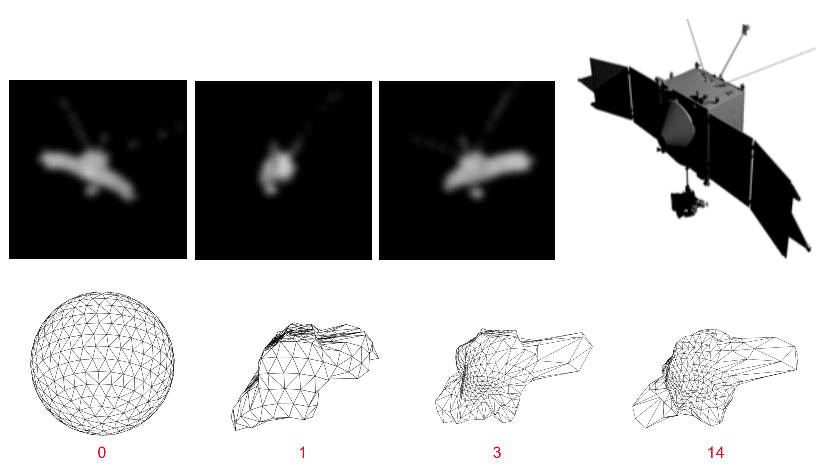

Figure 4: Shape from silhouette modeling with partially resolved images of the Maven spacecraft. Maven 3D model is from `https://nasa3d.arc.nasa.gov/models`. Synthetic images rendered using the open-source Blender software package, `https://www.blender.org`.

3 Summary of Results in Partially Resolved Object Recognition

We explored the feasibility of recognizing a space object given a set of partially resolved images. To do this, we require a representation of the object that serves as the bridge between the images and the catalog of known objects (Fig. 5). There are at least two ways to address this problem. The first is the explicit, hand-crafted construction of metrics and checks within a recognition pipeline. The second is a machine learning approach. We attempted both, and results are as follows.

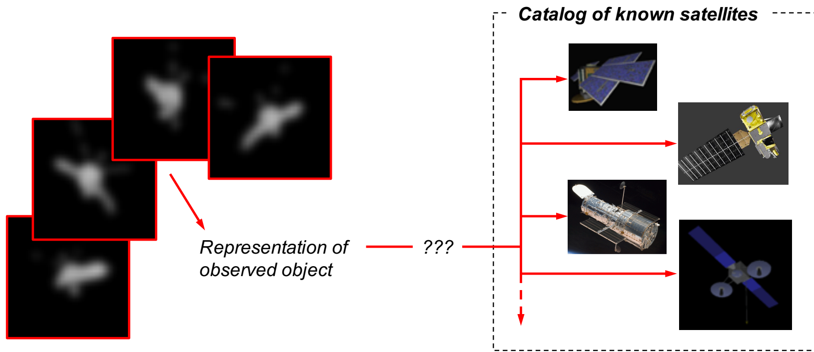

Figure 5: Space object recognition requires a common method of object representation to connect partially resolved images to a catalog of known objects.

3.1 Graph-based Keypoint Matching

We first explored the explicit construction of a recognition pipeline using the scale-space and keypoint localization results from Section 2.1. The relative location and scale of an object's keypoints represent a unique "fingerprint" for that object that may be used for matching. Specifically, we may reinterpret the set of keypoints as a graph. Each vertex pair in this graph has an edge whose value is chosen to be the Euclidean distance between the two vertices. Each vertex is assigned a value equal to its scale. This description of the keypoints is the same regardless of the frame in which it is represented (e.g., object frame, sensor frame) — this facilitates straightforward matching. We adapted a graph matching approach first developed by our research group for LIDAR reflector identification [23] to this problem and find it to work quite well. An example is shown in Fig. 6.

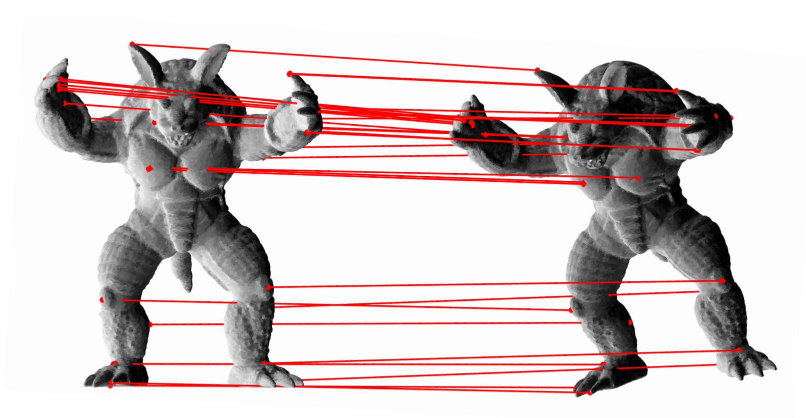

Figure 6: Graph-based matching of keypoints on two different meshes of the the Armadillo model. The catalog of keypoints included graphs for many objects (not just the Armadillo). The algorithm correctly identified the measured mesh (right) as the Armadillo and matched the corresponding keypoints.

3.2 Neural Networks

We also developed a machine learning pipeline for the recognition of partially resolved space objects using a convolutional neural network. Our neural network consisted of convolutional layers, max pool layers, and fully connected layers, organized in the manner shown in Fig. 7. This proof-of-concept network was trained on a catalog 14 objects (7 satellites and 7 asteroids) at phase angles from 0–138 deg. Images were grouped in to five different phase angle bins (since phase angle is strongly affects appearance and is almost always known in practice), with examples shown in Fig. 8. The success rate of correct object identification is found to be above 90% for both crisp and blurry images of objects known to the network.

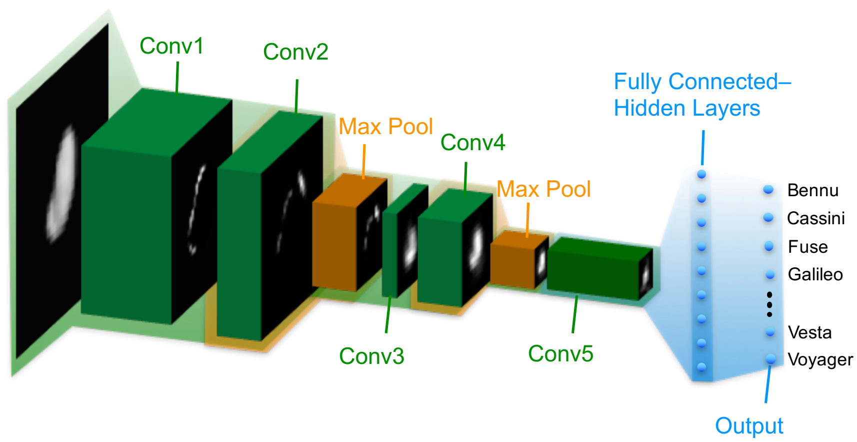

Figure 7: Illustration of our convolutional neural network (CNN) architecture for recognition of partially resolved space objects.

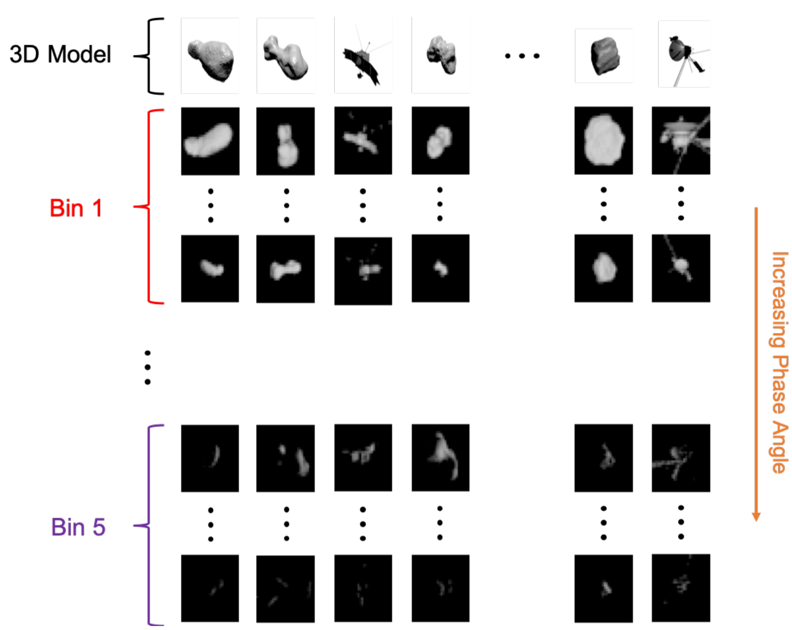

Figure 8: Illustration of the 14-object catalog, which is separated into five bins based on phase angle.

4 Summary of Results in Relative Navigation with Partially Resolved Objects

Vision-based spacecraft navigation is often reduced to producing a bearing to the object's center in situations where an object is not fully resolved. Algorithm simplicity often dictates that bearing be produced through a simple center-of-intensity (COI) algorithm. This approach generally works quite well for unresolved objects, but can produce a undesirably large bearing bias for partially resolved objects at a mid-to-large phase angles, g. This can be seen in Fig. 9, where the COI (red dot) is biased in the direction of illumination from the object's geometric center (blue dot).

During the course of this YIP award, we developed analytic expressions for the phase angle dependent bearing bias of a sphere with a constant illumination, a Lambertian reflectance model, and a Lommel-Seeliger reflectance model. We note that bias corrections for the sphere are not new [24], although study of the sphere allowed us to develop a framework that easily extends to other shapes. We generally explored the efficacy of analytic bearing bias correction with various geometric primitives, although the period of performance expired before we could run many of these issues to ground. With the YIP now over, this line of work is continuing under new sponsorship by NASA (where we are exploring specific geometric shapes and configurations of relevance to them).

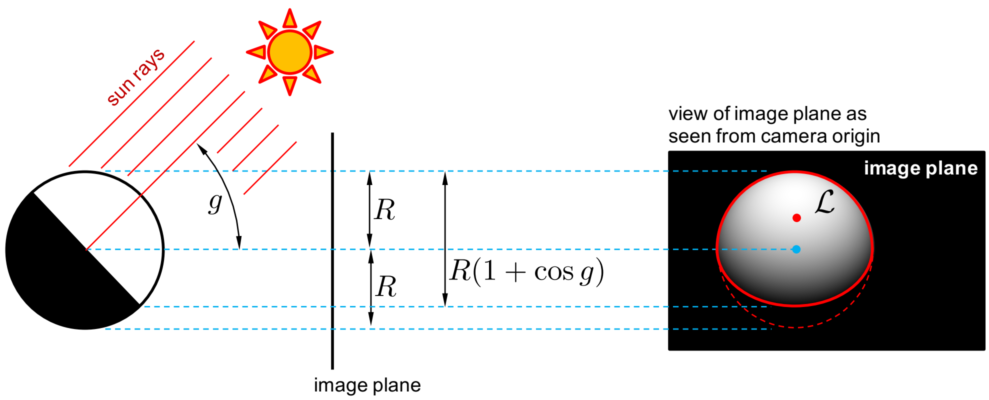

Figure 9: At non-zero phase angles, an object's center-of-intensity (COI) is generally biased away from its geometric center. This bias may be analytically computed for many common 3D shapes.

5 Publications

5.1 Conference Papers

The following conference papers have been written:

1. Kobylka, K., Puritz, J., and Christian, J., "Analytic Center of Illumination Solutions to Aid Relative Navigation with Partially Resolved Imagery," accepted for presentation at the AAS/AIAA Astrodynamics Specialist Conference, Portland, ME, 11-15 August 2019.
2. Ertl, C., Christian, J.A., "Identification of Partially Resolved Objects in Space Imagery with Neural Networks," Paper AAS 18-412, AAS/AIAA Astrodynamics Specialist Conference, Snowbird, UT, 19-23 August 2018.
3. Rhodes, A., Christian, J.A., "Constructing a 3D Scale Space from Implicit Surfaces for Vision-Based Spacecraft Relative Navigation," 41st Annual AAS Guidance, Navigation, and Control Conference, Paper AAS 18-016, Breckenridge, CO, 2-7 February 2018.
4. Jagat, A., and Christian, J.A., "Scale Selection for Vision-Based Relative Navigation using Scale Space Theory," AIAA/AAS Astrodynamics Specialist Conference, Long Beach, CA, 13-16 September 2016.
5. Jagat, A., and Christian, J.A., "Vision-Based Relative Navigation using 3D Scale Space Theory," Paper AAS 16-428, AAS Space Flight Mechanics Meeting, Napa, CA, 14-18 February 2016.

6. Flewelling, B., Murphy, T.S., Rhodes, A.P., Holzinger, M.J., and Christian, J.A., "Spatio-Temporal Scale Space Analysis of Photometric Signals with Tracking Error," Advanced Maui Optical and Space Surveillance Technology (AMOS) Conference, Maui, HI, 15-18 September 2015.

5.2 Journal Papers

The following journal papers have been written:

1. Ertl, C., and Christian, J.A., "Identification of Partially Resolved Objects in Space Imagery with Convolutional Neural Networks," submitted to The Journal of the Astronautical Sciences.
2. Rhodes, A.P., and Christian, J.A., "Scale-Space Construction and Keypoint Detection on 3D Meshes using Discrete Laplacians," submitted to International Journal of Computer Vision (IJCV).

In addition to the above papers, we have produced many valuable results that have not yet found their way into a journal paper. The results are not sizable enough to warrant a standalone journal article and should (in Dr. Christian's opinion) be paired with related developments. We expect results on the following topics (whose development was supported under this YIP award) to appear in forthcoming journal papers in the next few years:

1. Object recognition through 3D keypoint matching using algorithms adapted from star trackers and LIDAR reflector identification. This will also appear in Andrew Rhodes's Ph.D. thesis.
2. Silhouette-based shape modeling and object recognition.

5.3 Student Theses

The bulk of the work within Andrew Rhodes's forthcoming Ph.D. dissertation was supported by this YIP award. Stacie Williams (former AFOSR program manager for this award, now at DARPA) is on Andrew Rhodes's Ph.D. committee.

6 Collaboration with DoD and Industry

This YIP award helped facilitate a fruitful collaboration with Dr. Brien Flewelling at AFRL/RV at Kirtland AFB in the 2015-2016 timeframe. Some of the results of this collaboration are captured in our joint AMOS paper (conference paper #6 from Section 5.1). Informal collaboration continued after Dr. Flewelling left AFRL in mid-2016, although these more recent collaborations have not resulted in any publications.

References

[1] Witkin, A. P., "Scale Space Filtering," *Proceedings of the Eighth International Joint Conference on Artificial Intelligence*, 1983, pp. 1019–1022.

[2] Babaud, J., Witkina, A. P., Baudin, M., and Duda, R. O., "Uniqueness of the Gaussian Kernel for Scale-Space Filtering," *IEEE Transactions on Pattern Analysis and Machine Intelligence*, Vol. PAMI-8, No. 1, January 1986.

[3] Jones, P. W., Maggioni, M., and Schul, R., "Manifold Parametrizations by Eigenfunctions of the Laplacian and Heat Kernels," *PNAS*, Vol. 105, No. 6, February 2008, pp. 1803–1808.

[4] Mokhtarian, F. and Mackworth, A. K., "A Theory of Multiscale, Curvature-Based Shape Representation for Planar Curves," *IEEE Transactions on Pattern Analysis and Machine Intelligence (TPAMI)*, Vol. 14, No. 8, August 1992, pp. 789–805.

[5] Lindeberg, T., "Scale-space theory: A basic tool for analysing [sic] structures at different scales," *Journal of Applied Statistics*, Vol. 2, No. 21, 1994, pp. 224–270.

[6] Lowe, D. G., "Distinctive image features from scale-invariant keypoints," *International Journal of Computer Vision*, Vol. 60, 2004, pp. 91–110.

[7] Zhang, H., "Discrete Combinatorial Laplacian Operators for Digital Geometry Processing," *Proc. SIAM Conference on Geometric Design and Computing*, 2004, pp. 575–592.

[8] Pinkall, U. and Poltheir, K., "Computing Discrete Minimal Surfaces and their Conjugates," *Experimental Mathematic*, Vol. 2, 1993, pp. 15–36.

[9] Desbrun, M., Meyer, M., Schröder, P., and Barr, A. H., "Implicit Fairing of Irregular Meshes using Diffusion and Curvature Flow," *SIGGRAPH 99 Conference Proceedings*, 1999, pp. 317–324.

[10] Belkin, M., Sun, J., and Wang, Y., "Discrete Laplace Operator on Meshed Surfaces," *SCG Symposium on Computational Geometry*, 2008, pp. 278–287.

[11] Wardetzky, M., Mathur, S., Kalberer, F., and Grinspun, E., "Discrete Laplace Operators: No Free Lunch," *Eurographics Symposium on Geometry Processing*, July 2007, pp. 33–37.

[12] Sporring, J., Nielsen, M., Florack, L., and Johansen, P., editors, *Gaussian Scale Space Theory*, Vol. 8, Kluwer Academic Publishers, 1997.

[13] Osher, S. and Sethian, J. A., "Fronts Propagating with Curvature Dependent Speed: Algorithms Based on Hamilton-Jacobi Formulations," *Journal of Computational Physics*, Vol. 79, 1998, pp. 12–49.

[14] Mauch, S., *Efficient Algorithms for Solving Static Hamilton-Jacobi Equations*, Ph.d., California Institute of Technology, April 2003.

[15] Merriman, B. and Ruuth, S., "Diffusion Generated Motion of Curves on Surfaces," *Journal of Computational Physics*, Vol. 225, 08 2007, pp. 2267–2282.

[16] MacDonald, C. B. and Ruuth, S. J., "The Implicit Closest Point Method for the Numerical Solution of Partial Differential Equations on Surfaces," *SIAM Journal of Scientific Computing*, Vol. 31, No. 6, 2009, pp. 4330–4350.

[17] Mikolajczyk, K., *Detection of local features invariant to affine transformations*, Ph.D. thesis, Institut National Polytechnique de Grenoble, 2002.

[18] Zaharescu, A., Boyer, E., and Horaud, R., "Keypoints and Local Descriptors of Scale Functions on 2D Manifolds," *International Journal of Computer Vision*, Vol. 100, May 2012, pp. 78–98.

[19] Zou, G., Hua, J., Dong, M., and Qin, H., "Surface Matching with Salient Keypoints in Geodesic Scale Space," *Computer Animation and Virtual Worlds*, Vol. 19, 2008, pp. 399–410.

[20] Gaskell, R., Saito, J., Ishiguro, M., Kubota, T., Abe, T. H. N. H. S., Barnouin-Jha, O., and Scheeres, D., "Itokawa Shape Model V1.0. HAY-A-AMICA-5-ITOKAWASHAPE-V1.0," `https://sbn.psi.edu/pds/resource/itokawashape.html`, 2008, NASA Planetary Data System, 2008.

[21] Franco, J. and Boyer, E., "Efficient polyhedral modeling from silhouettes," *IEEE Transactions on Pattern Analysis and Machine Intelligence*, Vol. 31, No. 3, 2009, pp. 414–427.

[22] Mokhtarian, F. and Bober, M., *Curvature Scale Space Representation: Theory, Applications and MPEG-7 Standardization*, Kluwer Academic Publishers, 2003.

[23] Ertl, C., Christian, J. A., and Robinson, S., "Retro-Reflector Pattern Design and Identification for Orion Rendezvous, Proximity Operations, and Docking," *41st Annual AAS Guidance, Navigation, and Control Conference*, 2018.

[24] Kaasalainen, M. and Tanga, P., "Photocentre offset in ultraprecise astrometry: Implications for barycentre determination and asteroid modeling," Vol. 416, 2004, pp. 367–373.